2314–2319 Nucleic Acids Research, 1995, Vol. 23, No. 12

Stereochemistry-dependent bending in oligonucleotide duplexes induced by site-specific covalent benzo[a]pyrene diol epoxide-guanine lesions

Rong Xu, Bing Mao+, Jing Xu, Bin Li, Sheryl Birke, Charles E. Swenberg[1] and Nicholas E. Geacintov*

Chemistry Department, 31 Washington Place, New York University, New York, NY 10003, USA and [1]Radiation Biochemistry Department, Armed Forces Radiobiology Research Institute, Bethesda, MD 20814, USA

Received December 21, 1994; Revised and Accepted May 2, 1995

ABSTRACT

The apparent persistence length of enzymatically linearized pIBI30 plasmid DNA molecules ~2300 bp long, as measured by a hydrodynamic linear flow dichroism method, is markedly decreased after covalent binding of the highly tumorigenic benzo[a]pyrene metabolite *7R,8S*-dihydroxy-*9S,10R*-epoxy-7,8,9,10-tetrahydrobenzo[a]pyrene [(+)-*anti*-BPDE]. In striking contrast, the binding of the non-tumorigenic, mirror-image *7S,8R,9R,10S* enantiomer [(–)-*anti*-BPDE] to DNA has no measurable effect on its alignment in hydrodynamic flow gradients (≤2.2% of the DNA bases modified). In order to relate this effect to BPDE-nucleotide lesions of defined stereochemistry, the bending induced by site-specifically placed and stereochemically defined (+)- and (–)-*anti*-BPDE-N^2-dG lesions in an 11mer deoxyoligonucleotide duplex was studied by ligation and gel electrophoresis methods. Out of the four stereochemically isomeric *anti*-BPDE-N^2-deoxyguanosyl (dG) adducts with either (+)-*trans*, (–)-*trans*, (+)-*cis*, and (–)-*cis* adduct stereochemistry, only the (+)-*trans* adduct gives rise to prominent bends or flexible hinge joints in the modified oligonucleotide duplexes. Since both *anti*-BPDE enantiomers are known to bind preferentially to dG (≥85%), these observations can account for the differences in persistence lengths of DNA modified with either (+)-*anti*-BPDE or the chiral (–)-*anti*-BPDE isomer.

INTRODUCTION

Polycyclic aromatic hydrocarbons, e.g. benzo[a]pyrene (BP), are metabolized *in vivo* to potent genotoxic diol epoxide derivatives that covalently bind to DNA (1–3). The resulting distortions in the native DNA conformation are believed to adversely affect the cellular processing of the modified DNA, and play an important role in mutagenesis (4,5), as well as in the initiation stages of tumorigenesis (6). The most tumorigenic metabolite of BP is the stereoisomer *7R,8S*-dihydroxy-*9S,10R*-epoxy-7,8,9,10-tetrahydrobenzo[a]pyrene [(+)-*anti*-BPDE]; interestingly, the mirror image *7S,8R,9R,10S* enantiomer [(–)-*anti*-BPDE] is not tumorigenic (7,8). The mutagenic activities of these two enantiomers are also strikingly different, the (+)-isomer being more mutagenic in mammalian cells, while the (–)-enantiomer is more active in bacterial cells (9–11). The molecular and structural origins of the differences in biological activities of (+)- and (–)-*anti*-BPDE have long been of interest (12,13). Both enantiomers react predominantly by opening of the epoxide ring at the C10 position of BPDE and by either *trans* or *cis* addition of the exocyclic amino group of guanine residues in DNA (14,15); the stereochemical properties of the four possible BPDE-N^2-dG lesions are depicted in Figure 1. The availability of site-specifically modified oligonucleotides with stereochemically different BPDE-N^2-dG lesions, has made possible a number of conformational (16–18), spectroscopic (19), thermodynamic (20,21), biochemical (22) and site-directed mutagenesis studies *in vitro* (23–25) and *in vivo* (26).

Structural alterations, such as the induction of bends or hinge joints at the sites of the lesions, may constitute significant forms of DNA damage (27,28). These structural distortions may affect recognition of the damaged DNA by repair enzymes, and adversely influence replication and transcription. Using transient electric linear dichroism and gel electrophoresis methods, Hogan *et al.* (29) demonstrated that the covalent binding of racemic *anti*-BPDE to 145–185 bp DNA fragments induces bends or kinks. The covalent binding of the (+)-*anti*-BPDE enantiomer to native DNA reduces its apparent persistence length, as measured by hydrodynamic flow linear dichroism techniques (30,31). While BPDE–deoxyguanine adducts are dominant, the BPDE–DNA adduct distribution is heterogeneous (15) and the loss in persistence length (30,31) cannot be directly associated with any of the stereochemically distinct guanine adduct forms (Fig. 1). In order to assess the effects of stereochemically different *anti*-BPDE-N^2-dG lesions on bending, we synthesized BPDE-modified deoxyoligonucleotides with site-specifically placed BPDE-N^2-dG lesions of defined stereochemistry. Using ligation

* To whom correspondence should be addressed

+Present address: Cellular and Biophysics Program, Memorial Sloan-Kettering Cancer Center, 1275 York Avenue, New York, NY 10021, USA

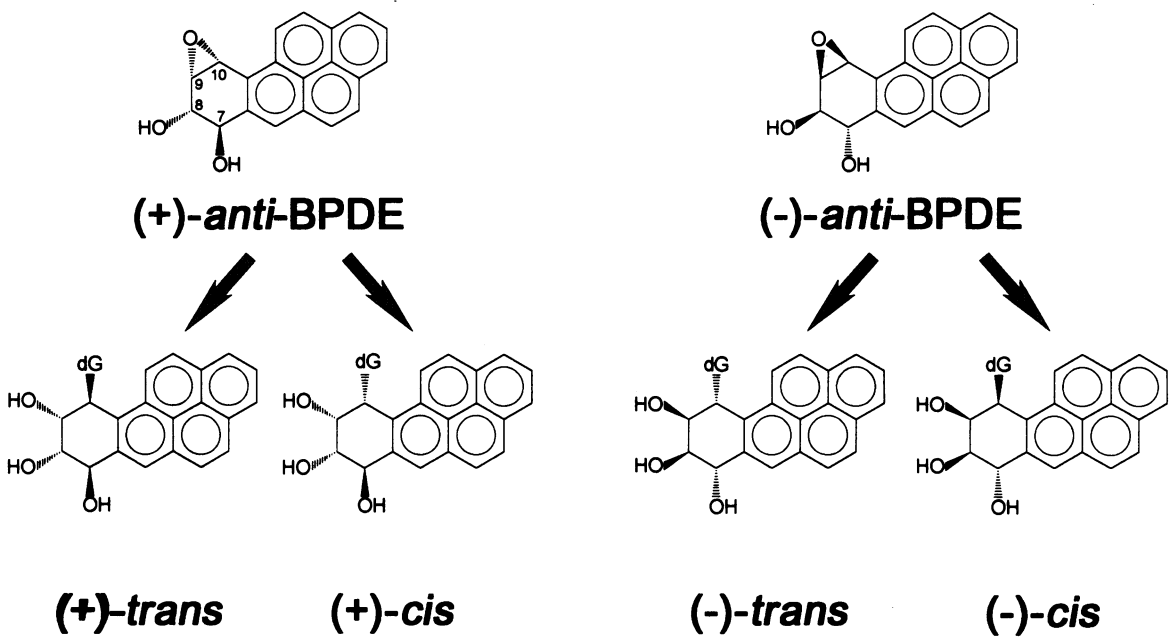

Figure 1. Stereochemistry of adducts resulting from the *trans*- or *cis*-addition of the two BPDE enantiomers to the exocyclic amino group of deoxyguanosine residues (dG).

and polyacrylamide gel electrophoresis methods, the electrophoretic mobilities of four stereochemically distinct isomeric BPDE-modified oligonucleotide duplexes were compared to one another.

MATERIALS AND METHODS

Preparation of BPDE-modified oligonucleotides

The oligonucleotides 5′-d(CACATGTACAC) and the strand 5′-d(GGTGTACATGT) were prepared by the phosphoramidite method using an automated DNA synthesizer. The (+)- and (–)-*anti*-BPDE enantiomers were purchased from the National Cancer Institute Chemical Carcinogen Reference Standard Repository (Chemsyn Sciences, Inc., Lot numbers 90-253-14-33 and 89-236-14-07, respectively). The stereochemically defined BPDE-modified oligonucleotides 5′-d(CACAT(G^{BPDE})TACAC), with (G^{BPDE}) = (+)-*trans-anti*-BPDE-N^2-dG, (–)-*trans-anti*-BPDE-N^2-dG, (+)-*cis-anti*-BPDE-N^2-dG, or (–)-*cis-anti*-BPDE-N^2-dG, were prepared by direct synthesis methods (32). Their stereochemical characteristics were ascertained as described previously for this particular sequence (19).

Labeling, ligation and gel electrophoresis

About 2 μg of each unmodified and BPDE-modified oligonucleotide were 5′-end-labeled with [γ-^{32}P]ATP (New England Nuclear) using 6 U of T4 polynucleotide kinase (Gibco Biological Research Laboratories) as described previously (22). After labeling with [γ-^{32}P]ATP, 2 μl of 0.1 M cold ATP (Pharmacia) and an additional 6 U of T4 polynucleotide kinase were added, and the reaction was continued at 37°C for an additional hour. The labeled unmodified and BPDE-modified single-stranded oligonucleotides were repurified using denaturing 20% polyacrylamide gel electrophoresis (7 M urea). The end-labeled and purified oligonucleotides were mixed with complementary strands designed to produce cohesive single-stranded ends, heated at 70°C for 10 min, and allowed to cool slowly to 8°C overnight, thus forming duplexes. The basic procedure of Koo *et al.* (33), with minor modifications, was used for ligating the following oligonucleotide duplexes (complementary: modified strand ratio 1.3:1) with cohesive ends at each end:

```
5′-CACATG*TACAC
   TGTAC ATGTGG-5′
```

Briefly, ~0.5 μg of these double-stranded oligonucleotides were incubated in 50 μl of ligation buffer solution (25 mM Tris–HCl, 5 mM $MgCl_2$, 0.5 mM ATP and 0.5 mM dithiothreitol, pH 7.6) and 10 U of T4 ligase (Gibco Biological Research Laboratories) at 12°C for ≥24 h. The ligated multimers were subjected to electrophoresis on non-denaturing 8% polyacrylamide gels in 0.1 M Tris-borate (pH 8.3), 2.5 mM EDTA (TBE buffer) at 4°C. The relative intensities of each of the bands were analyzed using a BIORAD 250 imaging system (Biorad, Hercules, CA).

BPDE-modified native DNA and flow linear dichroism measurements

The 2926 bp *Eco*RI enzyme restriction fragments of the plasmid pIBI30 were prepared as described previously (34), and were used in the hydrodynamic flow linear dichroism experiments because of their defined and homogeneous size. The DNA was reacted with either (+)- or (–)-*anti*-BPDE to generate BPDE-modified DNA molecules as described earlier (35). Aqueous DNA solutions were subjected to a hydrodynamic flow gradient in a Couette cell, and the absorbance was measured with linearly polarized light as described in detail elsewhere (34,35). The linear dichroism signal (LD) is defined as $A_{//} - A_{\perp}$, where $A_{//}$ and $A_{\perp}$ are the absorbances corresponding to the light polarization being oriented parallel or perpendicular to the flow direction, respectively

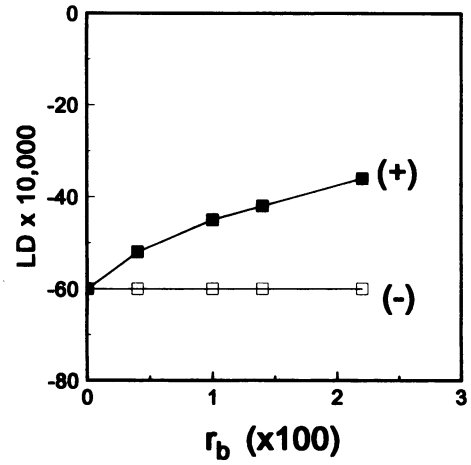

Figure 2. Linear dichroism signal measured at 260 nm of linearized pIBI30 fragments 2926 bp long covalently modified with (+)-BPDE (black squares) and (–)-BPDE (open squares) as a function of r_b, the fraction of modified bases. DNA concentration: 3.7×10^{-5} M (nucleotide concentration), in 5 mM Tris buffer solution (pH 7.9), 24 ± 1 °C. Flow gradient: 1800 s^{-1}. Additional details concerning the apparatus and methods of measurement are as previously described (34).

(36). The linear dichroism signal is proportional to the degree of alignment of the DNA molecules in the hydrodynamic flow gradient, and thus to the DNA persistence length (36).

RESULTS

Flow linear dichroism characteristics

The magnitude of the LD signal measured within the DNA absorption band at 260 nm is dominated by the DNA transition moments and thus reflects the degree of alignment of the DNA molecules. The DNA bases tend to align themselves with their planes perpendicular to the flow direction in the Couette cell, and the sign of the LD signal is thus negative at 260 nm (36).

The covalent binding of (+)-*anti*-BPDE causes increasingly large decreases in the magnitude of the LD signal with increasing r_b (number of BPDE residues/nucleotide) in the measured range of r_b = 0.004–0.022 (Fig. 2). These levels of binding correspond to one lesion per 25–125 bp, which are comparable with the average persistence length of unmodified native DNA [120–150 bp (37)]. In contrast to the effects caused by the (+)-stereoisomer, no observable changes in the hydrodynamic alignment of the (–)-*anti*-BPDE-modified DNA molecules up to r_b = 0.022 are observed (Fig. 2). Flow linear dichroism studies of (–)-*anti*-BPDE-modified calf thymus DNA were previously carried out only at low values of $r_b \leq 0.0037$), and the associated decrease in the LD signal was reported to be small (30). Our results span a wider range of r_b, and suggest that the adducts formed from (–)-*anti*-BPDE, unlike those derived from (+)-*anti*-BPDE, do not significantly perturb the overall persistence length of DNA. Although guanine residues are the major targets of binding of *anti*-BPDE in DNA, the adduct distribution is heterogeneous (15) and the bending effects cannot be directly and unambiguously associated with a particular lesion. However, the bending induced by stereochemically distinct *anti*-BPDE-N^2-dG lesions, can be examined by ligating site-specifically modified oligonucleotide duplexes, and by examining the electrophoretic mobilities of the ligation products on native polyacrylamide gels.

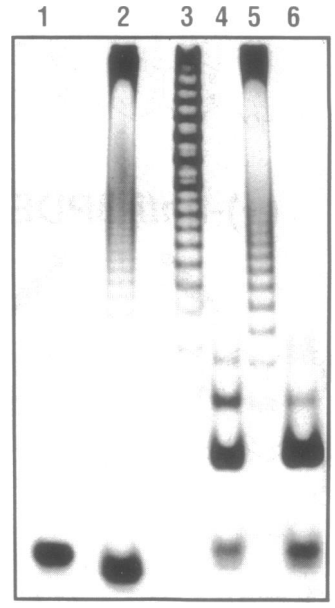

Figure 3. Ligation ladders of unmodified 11mer duplexes 5′-d(CACATGTACAC)•5′-d(GGTGTACATGT) (lane 2), and BPDE-modified duplexes 5′-d(CACAT(G^{BPDE})TACAC)•5′-d(GGTGTACATGT) with (+)-*trans*- (lane 3), (+)-*cis*- (lane 4), (–)-*trans*- (lane 5), and (–)-*cis*-adduct stereochemistry (lane 6). The single band in lane 1 is due to an unligated standard 11mer duplex used as a size marker (see text).

Gel electrophoresis of self-ligated oligonucleotides

A typical autoradiograph of a non-denaturing electrophoresis gel of ligation products of the BPDE-modified and unmodified 11mers is shown in Figure 3. Lane 1 represents the electrophoretic migration of an unmodified 11mer duplex 5′-d(CCATCGCTACC)•5′-d(GGGTAGCGATG) that is routinely used as a standard size-marker in our laboratory. Lane 2 represents the migration of a mixture of multimers of the ligated unmodified 11mer duplex 5′-d(CACATGTACAC)•d(GGTGTACATGT); lanes 3, 4, 5 and 6 represent electrophoretic mobility patterns of the ligation mixtures of the BPDE-modified duplexes 5′-d(CACAT(G^{BPDE})TACAC)•5′-d(GGTGTACATGT), with (G^{BPDE}) representing the (+)-*trans*- (lane 3), (+)-*cis*- (lane 4), (–)-*trans*- (lane 5), and (–)-*cis*-*anti*-BPDE-N^2-dG lesions (lane 6). In general, the appearance of these kinds of gels are variable, and depend not only on the ligation reaction time and the amount of enzyme, but also on the exposure time. The exposure of the photograph in Figure 3 was adjusted so as to emphasize the unusual set of dark bands in the upper portion of lane 3; some of the fainter, higher mobility bands are therefore poorly visible in this photograph. However, these fainter bands are evident in the densitometer tracings of lanes 2, 3 and 5 for the unmodified, (+)-*trans*-, and (–)-*trans*-BPDE-modified oligonucleotide duplexes (Fig. 4). Similar densitometer tracings were obtained with the (–)-*cis*- and (+)-*cis* oligomer adducts (lanes 4 and 6) that revealed a total of four and five variable-intensity bands, respectively (data not shown).

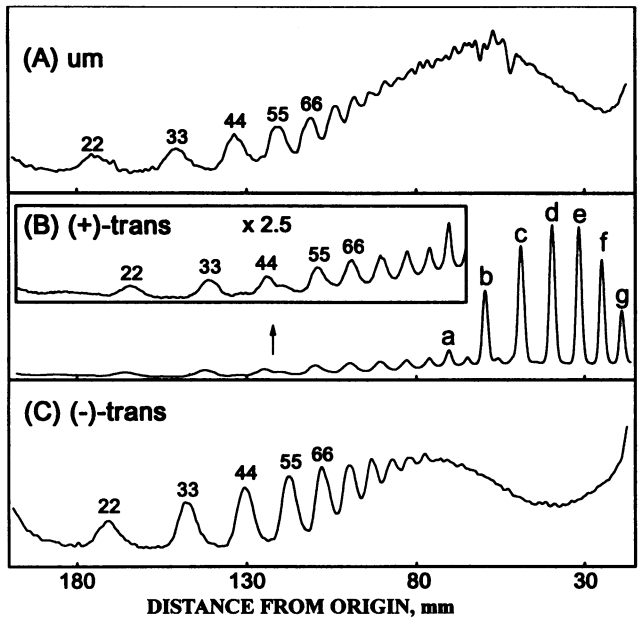

Figure 4. Densitometer tracings of lanes 2, 3 and 5 in Figure 3. (**A**) Unmodified (um) multimer duplexes (from lane 2 in Fig. 3). (**B**) (+)-*trans*-multimer adduct duplexes (from lane 3 in Fig. 3); the lower molecular weight portion corresponding to the normal progression of multimers is shown in the box at a 2.5× magnification. (**C**) (–)-*trans*-multimer adduct duplexes (from lane 5 in Fig. 3). The numbers above the bands denote the sequence lengths in base pairs. The circular DNA molecules are labeled 'a'–'g' (see text).

Remarkable adduct stereochemistry-dependent differences in the products of the ligation reactions are observed. These differences are summarized below.

Differences in [γ-^{32}P]ATP end-labeling and ligation efficiencies

A difference in [γ-^{32}P]ATP end-labeling efficiencies was noted during the course of these experiments. The efficiencies of labeling of *trans* and *cis* oligonucleotide adducts were about 40–50% and 70–80% as efficient, respectively, as the efficiency of labeling the unmodified 11mers. Thus, the amounts of labeled 11mers recovered in the five different samples (Fig. 3) were not entirely identical. Since identical amounts of complementary strands were added in each case, the actual ratio of complementary:labeled strands was highest in the case of the two *trans* adducts, and lowest in the case of the unmodified adducts. An excess of unligated 11mers is particularly pronounced at the bottom of lane 2 (Fig. 3); a closer analysis showed that these bands are mixtures of single-stranded and double-stranded unmodified 11mers (data not shown). The variable amounts of unligated 11mers in lanes 2, 4 and 6 (Fig. 3) are thus attributed, at least in part, to differences in the amount of labeled BPDE-modified strands recovered in the end-labeling experiments; this can lead to an insufficient excess of complementary strands, thus leading to partial dissociation of the duplexes, and inefficient ligation reactions.

High molecular weight ligation products are observed in all cases except in the cases of the two *cis* adducts (Fig. 3). In the case of the (+)-*trans*-BPDE adducts, much of the high molecular weight material is concentrated in six closely spaced intense bands at the top of lane 3 in Figure 3. There is a noticeable lack of higher molecular weight (+)-*cis*- and (–)-*cis*-multimer adducts (lanes 4 and 6 in Fig. 3). The ligation efficiencies of the (+)-*cis*- and (–)-*cis*-adduct duplexes are thus clearly lower than those of the unmodified and (+)-*trans*- and (–)-*trans*-adduct duplexes (lanes 4 and 5). The amount of *cis*-22mers is higher than the amount of 11mer or 33mers (lanes 4 and 6). These differences are greater than might be expected on the basis of a series of consecutive ligation reactions, each with similar rate constants. However, we noticed that the activity of the ligase decreases steadily during the course of the reactions; thus, quantitative comparisons of the amounts of different multimers formed is difficult, particularly with the slowly ligating *cis*-oligonucleotide adducts, and the origins of these effects were not further pursued. The differences in ligation efficiencies of the pairs of *trans* and *cis* oligonucleotide adducts may be associated with differences in adduct conformations. The *trans* adducts are characterized by external adduct conformations, while the *cis* adducts are intercalative in nature (19), as has been established for BPDE-N^2-dG in a similar sequence by high resolution NMR (16–18) and low resolution optical spectroscopic methods (21).

Electrophoretic mobilities

All of the oligonucleotide multimers containing BPDE residues migrate more slowly than the unmodified oligonucleotide multimers with the same number of base pairs, and thus are characterized by longer apparent sequence lengths. The slower mobilities of the BPDE-modified duplexes and their multimers as compared to the unmodified oligomers can be attributed, at least in part, to the additional mass of the BPDE residue. An examination of the densitometry traces (e.g. Fig. 4, and data not shown) indicate that the electrophoretic mobilities are arranged in the following order: unmodified > (–)-*trans* > (+)-*cis* ≳ (–)-*cis* > (+)-*trans* oligomers. The unusual relatively slow mobility of the (+)-*trans*-oligonucleotide adducts is revealed even more strikingly in plots of R_L versus the number of base pairs in each multimer (Fig. 5), where (33)

$$R_L = (\text{apparent length})/(\text{sequence length})$$

The apparent lengths of the BPDE-modified multimers are obtained by extrapolation of migration distances of a given BPDE-modified multimer band situated between two unmodified multimer bands of known sequence length. The migration distances are most easily evaluated from the densitometer tracings (e.g., Fig. 4).

The value of R_L is significantly greater, and its value increases more strongly as a function of increasing sequence length in the case of the (+)-*trans* adducts (Fig. 5). The larger R_L ratios are indicative of a greater degree of bending or of more prominent flexible hinge joints in (+)-*trans*-BPDE-modified duplexes than in the (–)-*trans*-, (+)-*cis*- and (–)-*cis*-BPDE-modified duplexes. The degree of bending associated with the multimers bearing the stereoisomeric (–)-*trans*-BPDE-N^2-dG lesions is apparently not sufficient to observe ring-closure, and minicircles are thus not observed in lane 4. From the data in Figure 3, no conclusions regarding minicircle formation can be reached in the case of the

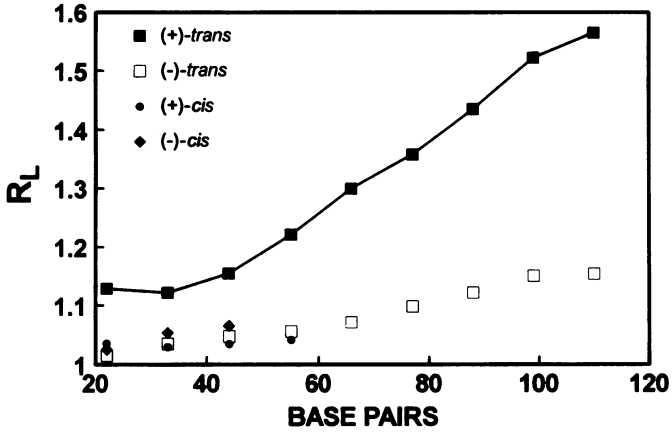

Figure 5. Plot of R_L-ratio as a function of sequence length, expressed in terms of the number of base pairs per DNA molecule.

two *cis* adducts, since the extent of ligation of the two *cis* adducts is insufficient.

Minicircle formation upon ligation of (+)-*trans* adducts

Much of the radioactivity is concentrated in the six prominent bands visible in the upper portion of lane 3 in Figure 3 (panel B in Fig. 4). Employing two-dimensional gel electrophoresis techniques (38,39), Mao has shown that these types of intense bands, which are observed only when (+)-*trans*-BPDE-modified oligonucleotide duplexes are ligated, are minicircles (40). Ring closure upon ligation is facilitated by bends and/or the flexibilities of the DNA molecules (41), and is thus a useful tool for studying the flexibilities and persistence lengths of DNA duplexes (42). Ongoing work on the characterization of these minicircles by known methods (38,39) shows that the size of the smallest minicircle is 77 bp (labeled 'a' in Fig. 4B), and that the six larger ones ('b'–'g') vary in size from 88 to 143 bp (Xu, R., Mao, B., Amin, S. and Geacintov, N.E., in preparation).

DISCUSSION

Correlation of reduced electrophoretic mobilities with alterations in hydrodynamic alignment of BPDE-modified native DNA fragments

When native DNA is reacted with either (+)-*anti*-BPDE or (–)-*anti*-BPDE, all four stereochemically possible adducts are formed in different proportions. In the case of the (+)-enantiomer, 94% are (+)-*trans*-BPDE-N^2-dG, 3% (+)-*cis*-adducts and 1% or less of the adducts involve binding to adenine residues. The adduct distribution generated by the (–)-*anti*-BPDE isomer is 58% (–)-*trans*-BPDE-dG, 5% (–)-*cis*-BPDE-N^2-dG and 15% (+)-*trans*-BPDE-N^6-dA adducts (15). The (+)-*trans*-BPDE-N^2-dG lesions outnumber all of the others by a factor of 20:1; thus, it may be assumed that the reduced alignment of (+)-*anti*-BPDE-modified DNA in hydrodynamic flow gradients (30,31) or transient electric fields (29), is associated with the dominant (+)-*trans*-BPDE-N^2-dG lesions.

Since the flow linear dichroism characteristics of (–)-*anti*-BPDE-modified DNA are not measurably affected in the same range of r_b (Fig. 2), we conclude that neither the (–)-*trans*- or (–)-*cis*-BPDE-N^2-dG, nor the (+)-*trans*-BPDE-N^6-dA lesions, significantly alter the persistence length of the modified DNA. The gel electrophoresis data is consistent with this conclusion since only oligonucleotide duplexes with (+)-*trans*-BPDE-N^2-dG lesions exhibit markedly slower electrophoretic mobilities than those containing any of the other three modified guanines. The gel electrophoresis studies presented here were obtained in a single sequence context. It will be of great interest to investigate the effects of base sequence on the nature of the bends (flexible versus static, degree of bending, etc.). Such investigations, especially the effects of bases flanking the modified Gs on circle size, are presently underway in our laboratory.

Finally, we note that structural distortions such as bends and flexible hinge joints induced by the covalent binding of drugs or bulky mutagenic and/or carcinogenic compounds are not uncommon. Examples of such ligands include 2-aminofluorene and its *N*-2-acetyl-derivative (27), (+)-CC1065 (43), cis-platin adducts (44), UV light-induced thymine dimers (45) and certain positional and configurational isomers of the polycyclic aromatic diol epoxide derivatives of 5-methylchrysene (34) and benz[a] anthracene (46).

ACKNOWLEDGEMENTS

This work was supported by the Office of Health and Environmental Research, the Department of Energy (DE-FGO2-86ER-60405). The synthesis of the BPDE-modified oligonucleotides was supported by Grant CA 20851 from the National Cancer Institute, National Institutes of Health.

REFERENCES

1 Singer, B. and Grunberger, D. (1983) *Molecular Biology of Mutagens and Carcinogens,* Plenum Press, NY.
2 Harvey, R.G., *Polycyclic Aromatic Hydrocarbons: Chemistry and Carcinogenicity,* Cambridge University Press, 1991.
3 Conney, A.H. (1982) *Cancer Res.* **42**, 4875–4917.
4 Rodriguez, H. and Loechler, E.L. (1993) *Carcinogenesis* **14**, 373–383.
5 Rodriguez, H. and Loechler, E.L. (1993) *Biochemistry* **32**, 1759–1769 (1993).
6 Harris, C.C. (1991) *Cancer Res. (Suppl.)* **51**, 5023s–5044s.
7 Buening, M.K., Wislocki, P.G., Levin, W., Yagi, H., Thakker, D.R., Akagi, H., Koreeda, M., Jerina, D.M. and Conney, A.H. (1978) *Proc. Natl. Acad. Sci. USA* **75**, 5358–5361.
8 Slaga, T.J., Bracken, W.J., Gleason, G., Levin, W., Yagi, H., Jerina, D.M. and Conney, A.H. (1979) *Cancer Res.* **39**, 67–71.
9 Wood, A.W., Chang, R.L., Levin, W., Yagi, H., Thakker, D.R., Jerina, D.M. and Conney, A.H. (1977) *Biochem. Biophys. Res. Commun.* **77**, 1389–1396.
10 Stevens, C.W., Bouck, N., Burgess, J.A. and Fahl, W.E. (1985) *Mutation Res.* **152**, 5–14.
11 Brookes, P. and Osborne, M.R. (1982) *Carcinogenesis* **3**, 1223–1226.
12 Geacintov, N.E. (1988) In Yang, S.K. and Silverman, B.D. (eds) *Polycyclic Aromatic Hydrocarbon Carcinogenesis: Structure–Activity Relationships.* CRC Press, Boca Raton, FL, Vol. II, pp. 181–206.
13 Gräslund, A. and Jernström, B. (1989) *Q. Rev. Biophys.* **22**, 1–37.
14 Meehan, T. and Straub, K. (1979) *Nature* **277**, 410–412.
15 Cheng, S.C., Hilton, B.D., Roman, J.M. and Dipple, A. (1989) *Chem. Res. Toxicol.* **2**, 334–340.
16 Cosman, M., de los Santos, C., Fiala, R., Hingerty, B.E., Ibanez, V., Margulis, L.A., Live, D., Geacintov, N.E., Broyde, S. and Patel, D.J. (1992) *Proc. Natl. Acad. Sci. USA* **89**, 1914–1918.
17 de los Santos, Cosman, M., Hingerty, B.E., Ibanez, V., Margulis, L.A., Geacintov, N.E., Broyde, S. and Patel, D.J. (1992) *Biochemistry* **31**, 5245–5252.
18 Cosman, M., de los Santos, C., Fiala, R., Hingerty, B.E., Ibanez, V., Luna, E., Harvey, R.G., Geacintov, N.E., Broyde, S. and Patel, D. (1993) *Biochemistry* **32**, 4145–4155.

19 Geacintov, N.E., Cosman, M., Mao, B., Alfano, A., Ibanez, V. and Harvey, R.G. (1991) *Carcinogenesis* **12**, 2099–2108.
20 Cosman, M., Geacintov, N.E. and Amin, S. (1993). In Garrigues, P. and Lamotte, M. (eds) *Polycyclic Aromatic Compounds. Synthesis, Properties, Analytical Measurements, Occurrence and Biological Effects.* Gordon & Breach, Switzerland, pp. 1151–1158.
21 Ya, N.-Q., Smirnov, S., Cosman, M., Bhanot, S., Ibanez, V. and Geacintov, N.E. (1994) In R.H. Sarma and M.H. Sarma (eds) *Structural Biology: The State of the Art. Proceedings of the 8th Converstaion.* Adenine Press, Schenectady, NY, Vol. 2, pp. 349–366 (1994).
22 Mao, B., Li, B., Amin, S., Cosman, M. and Geacintov, N.E. (1993) *Biochemistry* **32**, 11785–11793.
23 Hruszkewycz, A.M., Canella, K.A., Peltonen, K., Kotrappa, L. and Dipple, A. (1992) *Carcinogenesis* **13**, 2347–2352.
24 Shibutani, S., Margulis, L.A., Geacintov, N.E. and Grollman, A.P. (1993) *Biochemistry* **32**, 7531–7541.
25 Choi, D.-J., Marino-Alessandri, D.J., Geacintov, N.E. and Scicchitano, D.A. (1994) *Biochemistry* **33**, 780–787.
26 Mackay, W., Benasutti, M., Drouin, E. and Loechler, E.L. (1992) *Carcinogenesis* **13**, 1415–1425.
27 Schwartz, A., Marrot, L. and Leng, M. (1989) *J. Mol. Biol.* **207**, 445–450.
28 Leng, M. (1990) *Biophys. Chem.* **35**, 155–163.
29 Hogan, M.E., Dattagupta, N. and Whitlock, J.P., Jr (1981) *J. Biol. Chem.* **256**, 4504–4513.
30 Eriksson, M., Nordén, B., Jernström, B. and Gräslund, A. (1988) *Biochemistry* **27**, 1213–1221.
31 Roche, C.J. Geacintov, N.E., Ibanez, V. and Harvey, R.G. (1989) *Biophys. Chem.* **33**, 277–288.
32 Cosman, M., Ibanez, V., Geacintov, N.E. and Harvey, R.G. (1990) *Carcinogenesis* **11**, 1667–1672.
33 Koo, H.-S., Wu, H.-M. and Crothers, D.M. (1986) *Nature* **320**, 501–506.
34 Balasta, L., Xu, R., Geacintov, N.E., Swenberg, C.E., Amin, S. and Hecht, S.S. (1993) *Chem. Res. Toxicol.* **6**, 616–624.
35 Xu, R., Birke, S., Carberry, S.E., Geacintov, N.E., Swenberg, N.E. and Harvey, R.G. (1992) *Nucleic Acids Res.* **20**, 6167–6176.
36 Norden, B., Kubista, M. and Kurucsev, T. (1992) *Q. Rev. Biophys.* **25**, 51–170.
37 Hagerman, P.J. (1988) *Annu. Rev. Biophys. Biophys. Chem.* **17**, 265–286.
38 Zahn, K. and Blattner, F.R. (1987) *Science* **236**, 416–422.
39 Ulanovsky, L., Bodner, M., Trifonov, E.N. and Choder, M. (1986) *Proc. Natl. Acad. Sci. USA* **83**, 862–866.
40 Mao, B. (1993) Ph.D. Dissertation, New York University.
41 Shore, D., Langowski, J. and Baldwin, R.L. (1981) *Proc. Natl. Acad. Sci. USA* **78**, 4833–4837.
42 Hagerman, P.J. and Ramadevi, V.A. (1990) *J. Mol. Biol.* **212**, 351–362.
43 Lin, C.H., Sun, D. and Hurley, L.H. (1991) *Chem. Res. Toxicol.* **4**, 21–26.
44 Bellon, S.F. and Lippard, S.J. (1990) *Biophys. Chem.* **35**, 179–188.
45 Wang, C.-I. and Taylor, J.S. (1991) *Proc. Natl. Acad. Sci.USA* **88**, 9072–9076.
46 Carberry, S.E., Geacintov, N.E. and R.G. Harvey (1989) *Carcinogenesis* **10**, 97–103.